

Roles for *fgf8* signaling in left–right patterning of the visceral organs and craniofacial skeleton

R. Craig Albertson*, Pamela C. Yelick*

Department of Cytokine Biology, The Forsyth Institute, and Department of Oral and Developmental Biology, Harvard School of Dental Medicine, 140 The Fenway, Boston, MA 02115, USA

Received for publication 13 October 2004, revised 19 April 2005, accepted 20 April 2005
Available online 1 June 2005

Abstract

Laterality is fundamental to the vertebrate body plan. Here, we investigate the roles of *fgf8* signaling in LR patterning of the zebrafish embryo. We find that *fgf8* is required for proper asymmetric development of the brain, heart and gut. When *fgf8* is absent, nodal signaling is randomized in the lateral plate mesoderm, leading to aberrant LR orientation of the brain and visceral organs. We also show that *fgf8* is necessary for proper symmetric development of the pharyngeal skeleton. Attenuated *fgf8* signaling results in consistently biased LR asymmetric development of the pharyngeal arches and craniofacial skeleton. Approximately 1/3 of zebrafish *ace/fgf8* mutants are missing Kupffer's vesicle (KV), a ciliated structure similar to Hensen's node. We correlate *fgf8* deficient laterality defects in the brain and viscera with the absence of KV, supporting a role for KV in proper LR patterning of these structures. Strikingly, we also correlate asymmetric craniofacial development in *ace/fgf8* mutants with the presence of KV, suggesting roles for KV in lateralization of the pharyngeal skeleton when *fgf8* is absent. These data provide new insights into vertebrate laterality and offer the zebrafish *ace/fgf8* mutant as a novel molecular tool to investigate tissue-specific molecular laterality mechanisms.

© 2005 Elsevier Inc. All rights reserved.

Keywords: Asymmetry; Kupffer's vesicle; Craniofacial; Visceral organ; *fgf8*; Zebrafish

Introduction

The Nodal “cassette” is a highly conserved signaling cascade that plays a critical role in establishing the left–right LR body axis across vertebrate classes (Fischer et al., 2002; Hamada et al., 2002; Long et al., 2003). Functioning early in development, *nodal*-related genes are asymmetrically expressed in the left lateral plate mesoderm (LPM), and induce downstream antagonists (*lefty1* and *lefty2*), and effectors (*pitx2*), which regulate LR asymmetric development of the brain and visceral organs (Hamada et al., 2002; Liang et al., 2000).

While the Nodal cassette is a well-characterized molecular module, the manner by which the initial asymmetric cues are relayed from the midline to the left LPM is less

well established. Recent attention has focused on monociliated node cells in directing LR patterning of the LPM (Essner et al., 2002; Hamada et al., 2002). Ciliated nodal cells have been identified in mice, chick, frogs and fish (Essner et al., 2002) and are thought to break symmetry via directed ciliary movements (Brueckner, 2001). Evidence in support of this model is provided by analysis of mutant mouse embryos lacking the KIF3B motor protein, which exhibit immotile nodal cilia and randomized organ LR asymmetry (Nonaka et al., 2002). Strikingly, this condition can be rescued by applying artificial fluid flow to mutant embryos (Nonaka et al., 2002). In the zebrafish, monociliated cells similar to those present in the mouse node are located within Kupffer's vesicle (KV) (Brueckner, 2001), a transient structure that originates from the dorsal forerunner cells (DFCs) of the involuting blastoderm (Cooper and D'Amico, 1996) and localizes to the ventral tail bud (Kimmel et al., 1995). Several recent studies have demonstrated a link between KV and LR patterning in zebrafish

* Corresponding authors. Fax: +1 617 262 4021.

E-mail addresses: calbertson@forsyth.org (R.C. Albertson), pyelick@forsyth.org (P.C. Yelick).

(Amack and Yost, 2004; Essner et al., 2005; Hashimoto et al., 2004).

Fibroblast growth factors (Fgfs) are intercellular signaling molecules that participate in a wide array of developmental processes including LR asymmetric development of the visceral organs (Boettger et al., 1999; Fischer et al., 2002; Meyers and Martin, 1999). Fgf8 signaling from the ventral midline has been implicated in regulating the Nodal cassette in the LPM. In birds and mammals, *fgf8* is initially expressed along the developing midline. In the chick, *fgf8* becomes localized to the right side of the node, where it inhibits *nodal* expression on the right side of the embryo (Boettger et al., 1999). In mammals, the role of *fgf8* seems to vary depending on the shape of the gastrulating embryo (Fischer et al., 2002). For example, the early rabbit embryo develops as a flat blastodisc, similar to that of chick and humans (Fischer et al., 2002), whereas rodents gastrulate as cup-shaped egg cylinders (Meyers and Martin, 1999). In the rabbit, *fgf8* functions in a similar manner as in chick, by inhibiting *nodal*-signaling on the right side of the embryo. In mice, however, *fgf8* acts by inducing the Nodal cassette on the left side of the embryo (Meyers and Martin, 1999). Why differences in the shape of the embryo should affect signaling downstream of *fgf8* remains a matter of speculation, but concomitant differences in gap junction-mediated intercellular communications (Levin and Mercola, 1998, 1999) have been postulated as one possibility (Fischer et al., 2002). A link between *fgf8* and the morphogenesis of monociliated nodal cells has not yet been investigated.

With few exceptions, most molecular studies of LR asymmetry have focused on defects in the heart and gut (but see Halpern et al., 2003; Long et al., 2003). Significantly less is known about the molecular bases of LR patterning in the head despite the recognized importance of neurological asymmetries for cognition and behavior (Bisazza and de Santi, 2003; Corp and Byrne, 2004; Galaburda et al., 1978; Ghirlanda and Vallortigara, 2004; Lazenby, 2002; Mercola and Levin, 2001). There is mounting evidence that at least some aspect of nodal signaling regulates brain asymmetry (Halpern et al., 2003; Long et al., 2003), consistent with the observation that individuals with complete *situs inversus* also exhibit anatomical asymmetries in the brain (Kennedy et al., 1999). However, there is also accumulating evidence that mechanisms that regulate laterality in the head and body are, to a certain degree, decoupled (Mercola and Levin, 2001; Zhu et al., 1999). For example, individuals with *situs inversus* still show left cerebral hemisphere language dominance and strong right-hand preference (Kennedy et al., 1999). Furthermore, mirror-image or “bookend” asymmetries observed in non-conjoined monozygotic twins appear to be restricted to traits above the neck, including hair whorl direction, hand preference, dental patterns and unilateral eye and ear defects (Levin, 1999). It has even been postulated that laterality decisions in the head might be linked to the head organizer (Mercola and Levin, 2001).

The genetic and molecular basis of craniofacial asymmetries is likewise poorly understood. Craniofacial malformations account for up to 70% of known birth defects and are often associated with asymmetries in dental, skeletal and soft tissues (Hall, 1999; Tiner and Quaroni, 1996). The broad phenotypic range associated with most asymmetrically expressed craniofacial syndromes, coupled with variable etiologies, has made the diagnosis and clinical treatment of facial asymmetries particularly challenging. The paucity of molecular studies focused on understanding the basis of facial asymmetries is also likely due to the lack of good animal models.

In this report, we investigate the role of *fgf8* signaling in mediating laterality fate decisions in the zebrafish. We show that approximately 60% of embryos lacking *fgf8* exhibit laterally defects in either the visceral organs or the pharyngeal skeleton. LR randomization of the viscera correlates with randomized nodal signaling in the lateral plate mesoderm. Asymmetric craniofacial development is correlated with asymmetric segmentation of the pharyngeal endoderm. Interestingly, we link the occurrence of both defects to the presence or absence of Kupffer’s vesicle (KV). Approximately 30% of *ace/fgf8* mutants are missing KV. Only mutants that lack KV express defects in visceral organ laterality, whereas only mutants that possess KV show asymmetric craniofacial development. These data suggest that KV is not only required for normal asymmetric development of the viscera, but also that in the absence of *fgf8*, this ciliated organ directs aberrant asymmetric development of the pharyngeal skeleton. In all, we offer the zebrafish *ace/fgf8* mutant as a novel molecular tool to study the relationships between molecular mechanisms regulating lateralization of various organ systems.

Materials and methods

Zebrafish husbandry and embryo collection

Zebrafish were maintained and bred at 28.5°C in a 14-h light/10-h dark cycle in the Forsyth Zebrafish Facility. Embryos were collected by natural mating of pair-wise crosses, and maintained at 28.5°C as described (Westerfield, 1995). For this study, we used mutants homozygous for the *ace^{ti282a}* allele, which encodes a point mutation in the 5′ splice site following exon 2 that causes a frame shift and premature stop codon that strongly inactivates Fgf8 signaling (Reifers et al., 1998), although Draper et al. (2001) found that there was residual *fgf8* message produced in *ace^{ti282a}* mutants. Mutants were easily identified morphologically at the 22 somite stage by the absence of the cerebellum, and confirmed by PCR. At earlier stages, the identities of *ace/fgf8* homozygous mutants (e.g., KV-embryo in Fig. 1) were later confirmed by allowing them to grow to an age where they could be distinguished morphologically from wild type (wt) siblings.

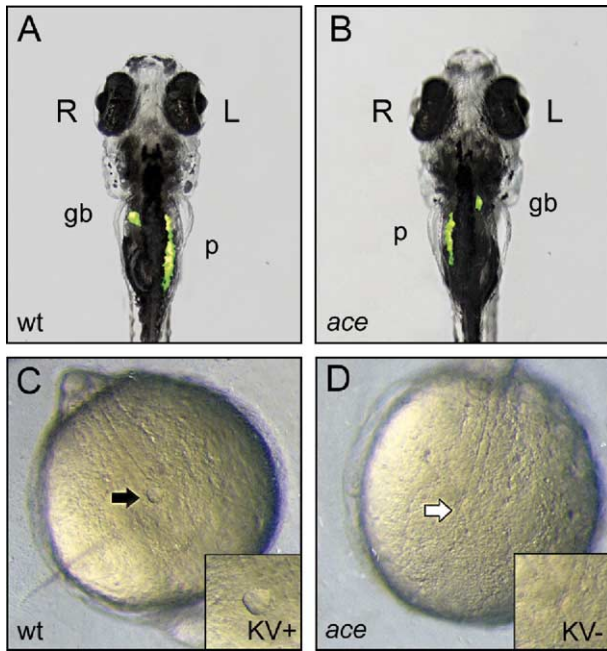


Fig. 1. *fgf8* is required for LR asymmetric development of the viscera and morphogenesis of Kupffer's vesicle (KV). (A–B) By 7 dpf the gall bladder (gb) and pancreas (p) autofluorescence under UV illumination, providing a simple screen for LR situs defects. (A) Wt larvae typically exhibit normal LR situs positioning (*situs solus*), with the gall bladder to the right of the midline and the pancreas to the left. (B) Approximately 30% of *ace/fgf8* mutants exhibit randomized LR situs positioning, including *situs inversus*. (C) KV is apparent in wt embryos by the five somite stage (black arrow). (D) KV does not develop in approximately 30% of *ace/fgf8* mutants (white arrow where KV should be).

Morpholino oligomer design and injection

Anti-sense morpholino oligomers (MO) (Gene Tools, LLC, Philomath, OR) targeted to the translational start site of *fgf8* were used: *fgf8*-MO, 5'-TGAGTCTCATGTTA-TAGCCTCAGT-3'. The standard control morpholino oligomer (SC-MO) was used as a negative control for the injection procedure (Gene Tools, LLC Philomath, OR). Nacre embryos (Lister et al., 1999) were injected with antisense morpholino oligomers (approximately 1–3 nl injection volumes) at the yolk/blastoderm interface of one to two-cell stage embryos at concentrations of 1.0, 2.0, 4.0 and 6.0 mg/ml in morpholino buffer (120 mM KCl, 20 mM HEPES–NaOH pH 7.5, 0.25% phenol red). Although craniofacial defects were observed in embryos injected with 2.0 mg/ml *fgf8* morpholino oligomer, larvae injected with 4.0 mg/ml exhibited craniofacial defects similar in severity, and laterality defects similar in frequency, as *ace/fgf8* mutants. Thus, the results reported here were obtained from embryos injected at 4.0 mg/ml concentrations.

Staining for cartilage and bone

The cartilages of 5 dpf larval fish were stained with Alcian blue (Ab) as described (Potthoff, 1984), with slight modification. Larvae were fixed overnight in 4% parafor-

maldehyde (PFA) in phosphate-buffered solution containing 0.1% Tween-20 (Sigma-Aldrich, St. Louis, MO). Larval cartilages were stained with 20 mg Ab (8XG Sigma-Aldrich, St. Louis, MO) in 65 ml glacial acetic acid and 35 ml absolute ethanol. After staining, specimens were enzymatically cleared using a trypsin solution containing 1 g of trypsin powder (Sigma-Aldrich, St. Louis, MO) in 65 ml distilled H₂O and 35 ml sodium borate saturated distilled H₂O, and stored in 80% glycerol. Bone was stained in 7 dpf larvae with a 0.1 mg/ml solution of the vital stain Quercetin (Sigma), and visualized under UV illumination using a Zeiss M2 Bio microscope. Cartilage and bone preparations were photographed using a Zeiss Axiocam digital imaging system and processed in Adobe Photoshop (v7). Asymmetric craniofacial development in *ace/fgf8* mutants was evaluated based on the gross presence/absence of cartilage and bone. Survival of *ace/fgf8* mutants was over 95% at 5 dpf and over 85% at 7 dpf. By 8 dpf survival dropped to below 60% ($n = 84$).

Whole-mount *in situ* hybridization (WISH) analysis

WISH analyses were performed on developmentally staged embryos using an adapted protocol (Sagerstrom et al., 1996; Thisse et al., 1993). Embryos were collected at desired stages, fixed in 4% PFA in phosphate-buffered solution containing 0.1% Tween 20, and dehydrated in methanol. Embryos were rehydrated, digested with 10 μ g/ml Proteinase K, and refixed in 4% PFA. Prehybridization was performed at 65°C for 3 h in 50% formamide, 5 \times SSC, 0.1% Tween-20, 4.6 mM citric acid, 50 μ g/ml Heparin and 500 μ g/ml tRNA. Digoxigenin-labeled anti-sense riboprobes (Roche Applied Science, Penzberg, Germany) were added directly to pre-hybridization mix and allowed to incubate overnight at 65°C. Riboprobes were synthesized from the following cDNAs: *dlx2* (Aki-menko et al., 1994); *fgf8* (Reifers et al., 1998); *ntl* (Schulte-Merker et al., 1994); *nkx2.3* (Chen and Fishman, 1996); *pitx2c* (Essner et al., 2000); and *spaw* (Long et al., 2003). Washes were performed the following day at 65°C in graded solutions from 100% hybridization mix to 100% 2 \times SSC, and then in 0.2 \times SSC. Embryos and α -dig antibody were pre-blocked at room temperature for at least 3 h in a solution containing 1 part 10% Boehringer blocking reagent dissolved in 1 M Maleic Acid, 1 part lamb serum and 3 parts filtered Maleic Acid Buffer (MAB: 100 mM Maleic Acid, 150 mM NaCl, 0.1% Tween 20, 7.9 g/L NaOH, pH to 7.5). After pre-blocking, embryos were transferred to the α -dig antibody solution and incubated overnight at 4°C. The following morning, embryos were washed first in MAB, and then in AP buffer solution (60 mM Tris–HCl pH to 9.5, 60 mM NaCl, 30 mM MgCl₂, and 0.1% Tween-20). Staining was achieved with NBT and BCIP in AP buffer. After staining, embryos were refixed in 4% PFA, dehydrated in 100% methanol overnight to remove background staining and stored in 80% Glycerol.

Results

ace/fgf8 mutants exhibit aberrant LR asymmetric development of the viscera

Embryos lacking *fgf8* exhibited randomized LR asymmetric development of the heart, gut and diencephalon (Table 1, Figs. 1 and 2). Contrary to a previous report (Chen et al., 1997), we found that both cardiac jogging and looping were affected in *ace^{tt282a}* mutants (Table 1A, and B). Similar to other zebrafish LR mutants exhibiting heart defects (e.g., *spt^{b104}*, *din^{tt250}* and *cyc^{b16}*) (Chen et al., 1997), we found that these processes were correlated in *ace/fgf8* mutants (e.g., embryos with a normal cardiac jog formed normal loops, whereas those with reversed or no jog formed reversed or no loops). At 26 hpf, wt zebrafish exhibited a normal jog to the left of the dorsal midline, whereas 30% of *ace/fgf8* mutants exhibited no cardiac jog, and another 14% exhibited a reversed jog to the right (Table 1A). By 48 hpf, wt zebrafish acquired a D-loop cardiac morphology with the ventricle bending to the right. At this stage, *ace/fgf8* mutants exhibited either no loop (42%), or a reversed L-loop (15%). Gut laterality was evaluated by observing the LR orientation of the gall bladder and pancreas in 7 dpf embryos under UV

illumination (Table 1C, Figs. 1A, B). In wt zebrafish, the gall bladder is oriented to the right of the midline and the pancreas is located on the left (Fig. 1A). Approximately 15–20% of *fgf8*-deficient larvae exhibited either reversed or midline positioning of the gall bladder and pancreas (Fig. 1B). Brain asymmetry was evaluated in wt and *ace/fgf8* mutants via asymmetric *pitx2c* expression in the dorsal diencephalon, as regulated by nodal signaling (Liang et al., 2000). At the 22 somite stage, wt embryos exhibited *pitx2c* expression on the left side of the diencephalon (Table 1D, Fig. 2G), while in age-matched *ace/fgf8* mutants, *pitx2c* expression was either absent (33%) or bilateral (38%) in the dorsal diencephalon (Table 1D, Figs. 2H, I).

The observed randomized asymmetric development of the heart, gut and brain in *ace/fgf8* mutants is likely due to aberrant nodal signaling in the LPM. The zebrafish nodal-related gene *southpaw* (*spaw*) is the earliest reported molecule to be asymmetrically expressed in the LMP and has been shown to be functionally important in asymmetric situs development (Long et al., 2003). In wt embryos, asymmetric *spaw* expression is first detected at the 12-somite stage in a narrow domain of the left LPM near the tail bud. By 20 somites, *spaw* expression has expanded antero-laterally and is strongly expressed in the left LPM of wt embryos

Table 1
fgf8 deficiency affects LR asymmetric development of the brain, heart and visceral organs

A. Cardiac jogging	Group	n	Heart jogging			
			% L-jog	% R-jog	% No jog	
	wt	80	99	0	1	
	<i>ace/fgf8</i>	80	56	14	30	
	SC-MO	25	100	0	0	
	<i>fgf8</i> -MO	35	40	25	35	
B. Cardiac looping	Group	n	Heart looping			
			% D-loop	% L-loop	% No loop	
	wt	27	100	0	0	
	<i>ace/fgf8</i>	88	43	15	42	
	SC-MO	25	95	0	5	
	<i>fgf8</i> -MO	32	42	25	33	
C. Position of the gall bladder and pancreas	Group	n	Visceral symmetry			
			% Normal	% Reversed	% Middle	
	wt	25	100	0	0	
	<i>ace/fgf8</i>	97	72	14	13	
	SC-MO	20	100	0	0	
	<i>fgf8</i> -MO	28	60	22	18	
D. <i>pitx2c</i> expression in the dorsal diencephalon	Group	n	<i>pitx2c</i> expression			
			% Normal	% Reversed	% Bilateral	% Absent
	wt	30	97	3	0	0
	<i>ace/fgf8</i>	58	29	0	38	33
E. <i>spaw</i> expression in the LPM	Group	n	<i>spaw</i> expression			
			% Normal	% Reversed	% Bilateral	
	wt	50	100	0	0	
	<i>ace/fgf8</i>	31	61	16	15	

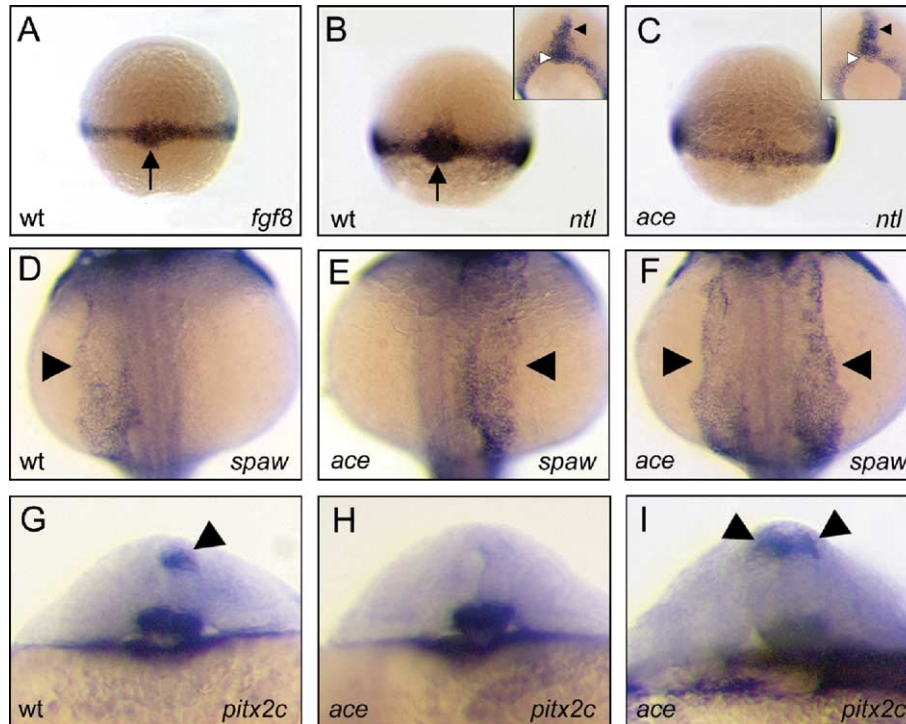


Fig. 2. (A, B) At shield stage, both *fgf8* and *ntl* mRNAs are expressed in wt dorsal forerunner cells DFCs (black arrows). (C) *ntl* expression is reduced in the margin and DFCs of age-matched *ace/fgf8* mutants. (B, C insets) By ~70% epiboly *ntl* expression in the midline of *ace/fgf8* mutants is indistinguishable from that in age-matched wt embryos (black arrowheads). (D–F) *fgf8* deficiency results in randomization of nodal signaling in the lateral plate mesoderm (LPM) (arrowheads). (D) The nodal-related gene *spaw* is expressed in the left LPM of wt embryos at 22 somites. Similarly staged *ace/fgf8* mutants exhibit reversed (E) and bilaterally (F) expressed *spaw* in the LPM. (G–I) Normal LR asymmetric development of the diencephalon is disrupted in *ace/fgf8* mutants (arrowheads). (G) At 26 hpf, *pitx2c* is expressed on the left side of the dorsal diencephalon. Expression of this marker is either absent (H) or bilateral (I) in *ace/fgf8* mutants.

(Table 1E, Fig. 2D). In contrast, expression of *spaw* in the LPM was either reversed (16%) or bilateral (15%) in *ace/fgf8* mutants (Table 1E, Figs. 2E, F). These data suggest that heart, brain and gut laterality defects observed in *fgf8* deficient zebrafish are due to randomized nodal signaling in the LPM.

fgf8 signaling is required for Kupffer's vesicle morphogenesis

To investigate the developmental origin of nodal-related laterality defects in *fgf8* deficient zebrafish, we examined Kupffer's vesicle (KV) morphogenesis. At shield stage (6 hpf), the wt zebrafish gastrula exhibited strong *fgf8* and *ntl* expression at the margin and in KV progenitors, the dorsal forerunner cells (DFCs) (Figs. 2A, B). In contrast, *ace/fgf8* mutants exhibited reduced *ntl* expression both at the margin, and in DFCs (Fig. 2C). By late gastrulation (>70% epiboly), through somitogenesis, *ntl* expression in the presumptive notochord of *ace/fgf8* mutants was indistinguishable from that of age-matched wt embryos (insets, Figs. 2B, C). Thus, aberrant LR asymmetric patterning in *ace/fgf8* mutants is likely not due to defective midline tissues. Rather, endogenous *fgf8* expression in the DFCs of wt embryos, and aberrant *ntl* expression in the DFCs of *ace/fgf8* mutants, implicates *fgf8* signaling in KV morphogenesis. Indeed, we found that KV was missing in approximately 30% of *ace/*

fgf8 mutant embryos ($n = 226$) (Fig. 1D), while KV was missing in only 1% of age-matched wt embryos ($n = 163$) (Fig. 1C). These data support a requirement for KV in normal LR asymmetric development of the viscera (Amack and Yost, 2004), and suggest that by regulating KV morphogenesis, *fgf8* is required at one of the earliest stages of LR patterning in the zebrafish embryo.

ace/fgf8 mutants exhibit craniofacial asymmetries

Cartilage development was examined in 132 *ace/fgf8* mutants at 5 dpf (Table 2A, Fig. 3). Nearly all mutants exhibited reduced numbers of posterior arch cartilages. Instead of five pairs of bilateral ceratobranchial (cb) cartilages normally present in wt larvae (Fig. 3A), *ace/fgf8* mutants typically possessed only four pairs (Fig. 3B). Approximately 35% (46/132) of mutants also exhibited distinct asymmetries in the number of cb cartilages present. In total, 54 cb cartilages were asymmetrically missing (mutants were often missing more than one cartilage). Seventy-six percent (41/54) of the asymmetrically missing cartilages were absent from the right side of the pharynx, a number significantly more than would be expected if both the right and left side were affected with equal probability ($\chi^2 = 14.5$, $P < 0.001$). Wild type embryos injected with *fgf8* morpholino oligomer exhibited the same frequency and directional bias of pharyngeal

Table 2
fgf8 deficiency affects laterality of craniofacial development

A. Pharyngeal cartilage asymmetry	Group	<i>n</i>	Cartilage symmetry		
			% Asymmetric mutants	% Right side missing	% Left side missing
	wt	50	0	–	–
	<i>ace/fgf8</i>	132	35	76	24
	SC-MO	48	0	–	–
	<i>fgf8</i> -MO	50	38	68	32
B. Pharyngeal bone asymmetry	Group	<i>n</i>	Bone symmetry		
			% Asymmetric mutants	% Right side missing	% Left side missing
	wt	30	0	–	–
	<i>ace/fgf8</i>	280	28	60	40
	SC-MO	40	0	–	–
	<i>fgf8</i> -MO	93	3	–	–
C. <i>dlx2</i> expression in the CNC	Group	<i>n</i>	<i>dlx2</i> expression		
			% Asymmetric mutants	% Right side missing	% Left side missing
	wt	35	0	–	–
	<i>ace/fgf8</i>	29	45	77	23
D. <i>nkx2.3</i> expression in the pharyngeal endoderm	Group	<i>n</i>	<i>nkx2.3</i> expression		
			% Asymmetric mutants	% Right side missing	% Left side missing
	wt	30	0	–	–
	<i>ace/fgf8</i>	27	52	79	21

cartilage asymmetries (Table 2A). Moreover, although the severity of observed craniofacial defects increased with increased concentration of injected *fgf8* morpholino oligomer (2.0–6.0 mg/ml), the frequency of cb cartilage asymmetry remained remarkably consistent (~35%). These observations suggest that the incomplete penetrance of craniofacial cartilage asymmetries in *ace/fgf8* mutants was not due to partial activity of wt Fgf8 protein.

We also observed distal branching of cb cartilages at different axial levels in *ace/fgf8* mutants, suggesting that the asymmetric defect was not limited to one pair of cb cartilages (Figs. 3C, D). The only posterior cartilage pair that was consistently unaffected was the fifth ceratobranchial (cb5), which was never missing or branched, and always bore the pharyngeal teeth. The pharyngeal teeth of *ace/fgf8* mutants were typically malformed, appearing smaller and less mature than age matched wt siblings. Although Fgf-mediated signaling is critical for tooth development in mammals (Thesleff et al., 1995), *fgf8* is not specifically expressed in the zebrafish developing tooth germ (Jackman et al., 2004). Thus, the irregular tooth development observed in *ace/fgf8* mutants may be due to secondary effects.

fgf8-dependent bone development was examined using in vivo Quercetin staining of mineralized tissues in 280 *ace/fgf8* mutant larvae at 7 dpf (Table 2B, Fig. 3). By 7 dpf, zebrafish normally possess a bilateral series of 11 pharyngeal bones (Fig. 3E). *ace/fgf8* mutant larvae exhibited

variable bone development, ranging from the complete absence of all bony elements, to the full complement of pharyngeal bones. The majority of *ace/fgf8* mutants were missing between 4 and 5 pharyngeal bones from each side of the pharynx (Fig. 3F). Twenty-eight percent (79/280) of *ace/fgf8* mutant larvae exhibited asymmetric pharyngeal bone development. Asymmetries were observed for both dermal and cartilage replacement bones derived from the first and second pharyngeal arches. However, asymmetries were most often associated with ventral bone constituents ($\chi^2 = 8.2$, $P = 0.003$) from the second pharyngeal arch ($\chi^2 = 49.8$, $P < 0.001$). The probability of asymmetric bone development did not correlate with the severity of craniofacial defects in *ace/fgf8* mutants. The total number of identified asymmetrically missing bones was 110, 60% (66/110) of these were missing from the right side of the pharynx, which was slightly more than expected if this were a fluctuating phenomenon ($\chi^2 = 3$, $P = 0.08$). Interestingly, only 3/93 (3%) *fgf8* morpholino-injected embryos exhibited asymmetric pharyngeal bone development, suggesting that *fgf8* deficient bone asymmetry may be determined later in development, after the time when larva have recovered from targeted protein depletion (Table 2B). The observation that bone asymmetry could not be elicited with *fgf8* morpholino injections (even at higher concentrations) suggests that different symmetry patterning mechanisms may exist for bone and cartilage derivatives.

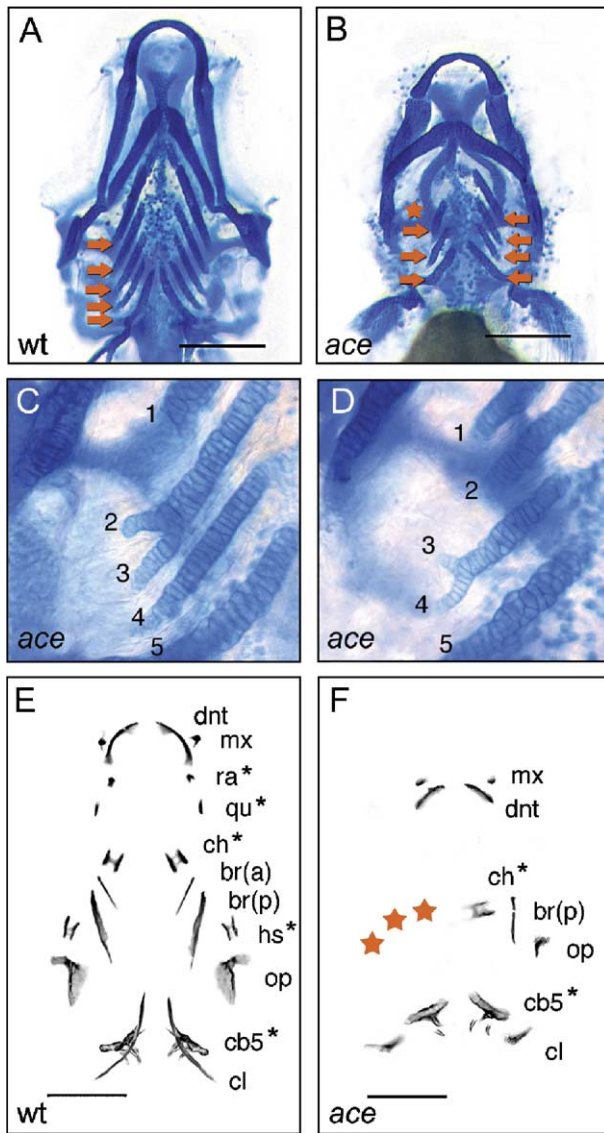


Fig. 3. Asymmetric craniofacial development in *ace/fgf8* mutants. All panels display a ventral view of the pharyngeal skeleton, with the right side of the pharynx present on the left, and the left side present on the right. (A) At 5 dpf, wt larvae exhibit five sets of paired bilateral cb cartilages (orange arrows). (B) Mutant larvae exhibit reduced and asymmetric numbers of cb cartilages (asterisk indicates position of asymmetrically missing cartilage). Pharyngeal cartilage asymmetry in *ace/fgf8* mutants has a directional bias with elements typically missing from the right side of the pharynx ($\chi^2 = 14.5$, $P < 0.001$). (C, D) *ace/fgf8* mutants exhibit lateral branching of various cb cartilages. (E, F) *ace/fgf8* mutants exhibit asymmetric pharyngeal bone development. (E) By 7 dpf, wt larvae possess a bilateral series of 11 mineralized bones. Pharyngeal bones are labeled to the right side of the figure (see abbreviations below). Starred bones represent cartilage replacement bones; all others are dermal bones. (F) Mutant larvae exhibit reduced and asymmetric bone development with a bias toward the right side of the pharynx ($\chi^2 = 3$, $P = 0.08$) (red asterisks indicate position of asymmetrically missing bones). Abbreviations are as follows: br(a), anterior branchiostegal ray; br(p), posterior branchiostegal ray; cb5, fifth ceratobranchial cartilage; ch, ceratohyal; cl, cleithrum; dnt, dentary; hs, hyosymplectic; mx, maxilla; op, opercle; qu, quadrate; ra, retroarticular.

Aberrant pharyngeal arch development may contribute to observed craniofacial asymmetry in ace/fgf8 mutants

Molecular analyses revealed pharyngeal arch defects in *ace/fgf8* mutants (Fig. 4). Pharyngeal arch segmentation in wt and mutant embryos was examined via *dlx2* expression in the cranial neural crest (CNC) of each pharyngeal arch (Table 2C, Figs. 4A–C). At 36 hpf wt larvae possessed a bilateral series of seven pharyngeal arches (Fig. 4A). In contrast, age-matched *ace/fgf8* mutants exhibited only 4–6 arches, and a subset of these mutants (45%) exhibited an asymmetric number of pharyngeal arch segments (Figs. 4B, C). In 77% of *ace/fgf8* mutants exhibiting asymmetric pharyngeal arch development, fewer arches were present on the right side of the pharynx, consistent with the right-sided bias of asymmetric pharyngeal arch cartilage development in *ace/fgf8* mutants. The expression of *dlx2* in *ace/fgf8* mutants also revealed instances where CNC segments appeared large and amorphous relative to those in wt larvae (Figs. 4B, C, versus A). This observation suggests that posterior pharyngeal arch CNC streams may have failed to separate in *ace/fgf8* mutants, leading to the same number of CNC cells occupying fewer endodermal pouches.

We also examined development of the pharyngeal endoderm via *nkx2.3* expression (Table 2D, Figs. 4D–F). At 32 hpf, wt zebrafish exhibited five discrete pharyngeal endodermal segments (Fig. 4D). In contrast, *ace/fgf8* mutants exhibited reduced and asymmetrical numbers of endodermal segments (Figs. 4E, F). Approximately half of *ace/fgf8* mutants showed asymmetric development of the pharyngeal endoderm ($n = 29$). Of these, 79% exhibited fewer segments on the right side, consistent with the right-sided bias of asymmetric CNC and craniofacial development in *ace/fgf8* mutants.

Segmentation of the zebrafish pharynx is a complex morphogenic process that involves coordinated development of pharyngeal endoderm and CNC (Crump et al., 2004). The zebrafish *van gogh* (*vgo*) mutant, for example, lacks pharyngeal endodermal pouches, and exhibits fused CNC segments and branched cb cartilages (Piotrowski and Nusslein-Volhard, 2000) similar to the defects we observed in *ace/fgf8* mutants. Our data support a model where disrupted *fgf8* signaling results in irregular pharyngeal arch segmentation and improper patterning of the pharyngeal endoderm, leading to the formation of fused, branched and variable numbers of ceratobranchial cartilages. The most striking observation is the consistent directional asymmetric bias of these defects.

Kupffer's vesicle is required for proper LR asymmetric development of the brain and viscera, and for lateralization of craniofacial development in the absence of fgf8

To explore the association of KV morphogenesis and laterality defects in *ace/fgf8* mutants, visceral (Table 3) and craniofacial (Table 4) development was examined in

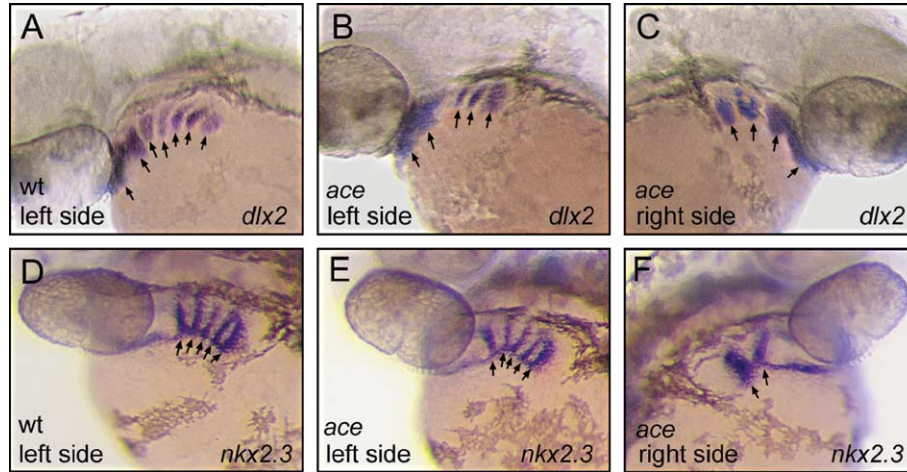


Fig. 4. *ace/fgf8* mutants exhibit asymmetric pharyngeal arch development. (A–C) Cranial neural crest (CNC) segments at 36 hpf in wt and mutant larvae (black arrows). (A) Wt *dlx2* expression in 7 bilateral CNC segments. (B, C) Age-matched *ace/fgf8* mutants exhibit fewer and often asymmetrical numbers of CNC segments. (D–F) Pharyngeal endoderm pouches in wt and mutant larvae (black arrows). (D) At 32 hpf, wt larvae possess a bilateral series of pharyngeal endodermal pouches, revealed via *nkx2.3* expression. (E, F) In some *ace/fgf8* mutants, the pharyngeal endoderm develops asymmetrically, with fewer endodermal pouches apparent on the right side of the pharynx.

embryos sorted by the presence or absence of KV. Mutants lacking KV expressed an equal probability of having normal (42%) or reversed (58%) positioning of the gall bladder and pancreas ($n = 50$). In contrast, the majority of KV(+) mutants (90%) expressed normal visceral LR asymmetric *situs* ($n = 106$) (Table 3A). Mutants lacking KV also exhibited randomized expression of genes involved in nodal signaling (Table 3B, C). Sixty-one percent of KV(–) mutants exhibited reversed or bilateral expression of *southpaw* (*spaw*) in the LPM ($n = 26$), and 71% of KV(–) embryos expressed randomized expression of *pitx2c* in the dorsal

diencephalon ($n = 27$). In contrast, the vast majority of KV(+) *ace/fgf8* mutants (97%–100%) exhibited normal asymmetric expression of *spaw* and *pitx2c* ($n = 38$ and 39 , respectively). It is worth noting that *ace/fgf8* mutants exhibited significant variation in the size of KV, compared to wt embryos, which could explain why 10% of mutants that were scored as KV(+) exhibited abnormal LR *situs*. Furthermore, it has been shown that zebrafish lacking a morphologically identifiable KV still possessed monocilia (Amack and Yost, 2004; Essner et al., 2005). The effects of both KV size and monocilia number on LR *situs* development are topics that remain to be explored in zebrafish.

Aberrant asymmetric development of the pharyngeal skeleton was only associated with *ace/fgf8* mutants that possessed KV (Table 4). Sixty-six percent of KV(+) mutants exhibited craniofacial asymmetries ($n = 151$), whereas only 2/43 (5%) of KV(–) mutants exhibited asymmetric craniofacial development (Table 4A). Similarly, asymmetric pharyngeal arch segmentation was only observed in KV(+) larvae. Nearly 40% of KV(+) mutants exhibited asymmetric *nkx2.3* expression ($n = 42$). In contrast, no

Table 3
Loss of Kupffer’s vesicle in *ace/fgf8* mutants affects normal LR asymmetric development of the viscera

A. Position of the gall bladder and pancreas	Group	n	Visceral symmetry	
			% Normal	% Randomized ^a
	<i>ace/fgf8</i> KV+	106	90	10
	<i>ace/fgf8</i> KV–	50	42	58

B. Nodal signaling in the LMP	Group	n	<i>spaw</i> expression	
			% Normal	% Randomized ^b
	<i>ace/fgf8</i> KV+	38	97	3
	<i>ace/fgf8</i> KV–	26	39	61

C. Development of the dorsal diencephalon	Group	n	<i>pitx2c</i> expression	
			% Normal	% Bilateral ^c
	<i>ace/fgf8</i> KV+	39	100	0
	<i>ace/fgf8</i> KV–	27	29	71

^a Randomized includes reversed and midline position.
^b Randomized includes reversed and bilateral expression.
^c Both KV– and KV+ mutants lacked *pitx2c* expression in the dorsal diencephalon with equal frequency. Only data on bilaterally expressed *pitx2c* is presented.

Table 4
Expression of craniofacial asymmetries in *ace/fgf8* mutants requires the presence of Kupffer’s vesicle

A. Development of the pharyngeal cartilage	Group	n	Cartilage development	
			Asymmetric	Symmetric
	<i>ace/fgf8</i> KV+	151	66%	34%
	<i>ace/fgf8</i> KV–	43	5%	95%

B. Segmentation of the pharyngeal endoderm	Group	n	<i>nkx2.3</i> expression	
			Asymmetric	Symmetric
	<i>ace/fgf8</i> KV+	42	38%	62%
	<i>ace/fgf8</i> KV–	28	0%	100%

KV(–) mutant larvae showed asymmetric expression of this marker ($n = 28$). It is important to note that both KV(–) and KV(+) *ace/fgf8* mutants exhibited similar craniofacial defects including an overall shortening of the pharyngeal skeleton and fewer cb cartilages; the key difference being that defects in KV(–) mutants were symmetrical, whereas those in KV(+) mutants were asymmetrical. A more thorough review of craniofacial defects in *ace/fgf8* mutants has been reported (Albertson and Yelick, 2004).

Discussion

Fgfs in LR patterning and craniofacial development

Fibroblast growth factors (Fgfs) participate in LR asymmetric patterning of the vertebrate embryo (Boettger et al., 1999; Creuzet et al., 2004; Crump et al., 2004; Fischer et al., 2002; Meyers and Martin, 1999; Walshe and Mason, 2003). Analyses in the mouse and chick have demonstrated that Fgf signaling from the embryonic midline regulates the Nodal cassette in the LPM. How these asymmetric cues are relayed from the midline to the LPM remains poorly understood. In this report, we have shown that zebrafish *fgf8* signaling is required for asymmetric expression of the Nodal cassette and development of the viscera possibly by supporting development of Kupffer's vesicle (KV). This hypothesis is supported by endogenous *fgf8* expression within the dorsal forerunner cells (DFCs) at shield stage, and by reduced *ntl* expression in DFCs when *fgf8* is absent. However, *fgf8* expression persists in the ventral tail bud during somitogenesis (data not shown). It is possible that *fgf8* signaling from the tail bud regulates nodal signaling in the LPM independent of KV. Future studies are required to determine whether *fgf8* regulates LR patterning of the zebrafish viscera directly via signaling from the ventral midline, indirectly through DFCs, or both.

Several genetic pathways have been identified that regulate left–right development of the brain and viscera in zebrafish (Bisgrove et al., 2000). Accordingly, zebrafish left–right mutants have been classified by altered patterns of asymmetric marker gene expression (Bisgrove et al., 2000). For example, Class I mutants exhibit predominantly bilateral expression of marker genes in the brain, heart field and gut (e.g., *ntl*^{b195}, *flh*ⁿ¹). Class II mutants exhibit bilateral, reversed and discordant gene expression in the brain, heart field and gut (e.g., *spt*^{b104}, *cas*^{ta56}). Class III mutants show bilateral and absent marker gene expression in the brain, and normal (left-sided) marker gene expression in the heart field and gut (e.g., *cyc*^{tf219}). Class IV mutants exhibit absent asymmetric marker gene expression (e.g., *oep*^{m134}), although *MZoep*^{m134} mutants exhibit both bilateral and absent asymmetric marker gene expression (Liang et al., 2000). Zebrafish *ace/fgf8* mutants exhibited both bilateral and reversed expression of the nodal-related gene *spaw* in the LPM, consistent with patterns observed in Class

II mutants. In contrast, *pitx2c* expression in the dorsal diencephalon was either absent or bilateral (but not reversed) in *ace/fgf8* mutants, which is more consistent with Class III mutants. Unfortunately, the stages of asymmetric expression of *spaw* and *pitx2c* are slightly out of phase, which made it difficult to assess LMP and diencephalic defects in the same embryos. However, in a small number of embryos we were able to score marker gene expression in the brain and LPM simultaneously, and found discordant defects in these regions, suggesting that *fgf8* may be functioning in different genetic pathways in the head and body. Additional asymmetrically expressed marker genes need to be examined in more embryos before the degree of autonomy between *fgf8*-dependent laterality in the brain and LPM may be determined.

The absence of asymmetric *pitx2c* expression in the dorsal diencephalon also occurred independent of the presence of KV. This observation suggests that *fgf8* has two functions in brain development, one in early asymmetric expression of *pitx2c* via KV morphogenesis, and the other in later development of the dorsal diencephalon, which is KV-independent. In zebrafish, the dorsal diencephalon gives rise to the pineal organ, which will induce asymmetric development of the parapineal and dorsal habenular nuclei (reviewed by Halpern et al., 2003). A role for zebrafish *fgf8* in the development of the pineal organ has not been investigated. However, sustained expression of *fgf8* in the dorsal diencephalon/pineal domain from 14 somite stage (16 hpf) through long-pec stage (60 hpf) (Thisse et al., 2001), and observations reported here in *ace/fgf8* mutants, support a role for *fgf8* in the development of the zebrafish pineal domain.

Fgfs also participate in several cellular processes during craniofacial development. It was recently shown that *fgf8* regulates proliferation, migration, and survival of CNC cells in the chick (Creuzet et al., 2004). We found little evidence for elevated levels of apoptosis during craniofacial development in *ace/fgf8* mutants (data not shown). Cell survival was certainly not effected to the degree that was reported for *fgf3*-deficient zebrafish (Walshe and Mason, 2003). Fgfs have also been shown to support mesoderm formation and pharyngeal endoderm segmentation in the zebrafish (Crump et al., 2004; Reifers et al., 2000). A model was recently proposed in which Fgfs coordinate craniofacial development via early signaling from the mesoderm and brain to promote pharyngeal (endodermal) pouch formation, and later from the pharyngeal endoderm to promote CNC survival (Crump et al., 2004). These studies underscore the complexity and importance of Fgfs in vertebrate craniofacial development.

It is clear from this work that zebrafish *fgf8* participates in at least two laterality pathways: one during early LR situs development, and another during later craniofacial development. We show that both mechanisms are associated with the presence of KV. A role for KV in establishing laterality of the brain and viscera has been demonstrated previously (Amack and Yost, 2004; Essner et al., 2005), but a role for

KV in establishing latent handedness in superficially paired structures has gone unnoticed until now. We show that when KV is present, visceral and craniofacial asymmetry is gained in *ace/fgf8* mutants. Conversely, when KV is absent, these asymmetries are lost. Thus, KV appears capable of lateralizing tissues as disparate as the gut and pharyngeal skeleton. These observations suggest that *fgf8* may act to suppress latent asymmetry (possibly determined by KV) during craniofacial development, making the zebrafish *ace/fgf8* mutant an important resource to explore molecular mechanisms of KV mediated lateralization.

The partial penetrance of laterality defects observed in *ace/fgf8* mutants could be due to compensatory activity of other *fgfs*. For example, zebrafish *fgf24* is co-expressed with *fgf8* in mesodermal precursors during gastrulation, and has been shown to function with *fgf8* to promote development of the posterior mesoderm (Draper et al., 2003). Furthermore, *fgf8* is co-expressed with both *fgf24* and *fgf3* in the pharyngeal arches, and with *fgf3* in the midbrain/hindbrain boundary (mhb) and rhombomere 4 (Crump et al., 2004; Draper et al., 2003; Walshe and Mason, 2003). Both *fgf8* and *fgf3* are required for pharyngeal arch segmentation and subsequent pharyngeal cartilage development (Crump et al., 2004; Walshe and Mason, 2003). The effects of knocking down the function of multiple Fgfs on LR development of the visceral organs and pharyngeal skeleton will be explored in future studies.

A genetic basis for naturally occurring and clinical craniofacial asymmetries

Craniofacial malformations account for ~70% of known birth defects (Hall, 1999), and several of the most common are characterized by asymmetries in dental, skeletal and soft tissues. In stark contrast to the mounting body of literature focused on molecular mechanisms regulating LR asymmetric development of visceral organs, very little is known about the molecular cues that establish the LR axis during craniofacial development. A genetic basis for naturally occurring directional craniofacial asymmetry is supported by heritability estimates and mapping studies in human and animal populations (Cassidy et al., 1998; Leamy et al., 2000). Investigations of clinical craniofacial asymmetries have recently been bolstered by the development of mutant mouse models for two of the most common malformations characterized by facial asymmetries. Hemifacial microsomia (HFM) affects first and second arch derivatives and is the second most common craniofacial disorder after cleft lip and palate with an estimated incidence of 1 in 3500 to 5600 live births (Tiner and Quaroni, 1996). The HFM mouse mutant was identified as a loss-of-function mutation at locus B3 on mouse chromosome 10, and termed the “hemifacial microsomia-associated” locus or *Hfm* locus (Naora et al., 1994), although the molecular nature of the mouse *Hfm* locus remains uncharacterized at this time. Treacher–

Collins Syndrome (TCS), an autosomal dominant disorder that affects the first and second arch, has an estimated incidence of 1 in 10,000 live births (Tiner and Quaroni, 1996). The TCS mouse mutant was generated via targeted mutagenesis of the mouse *Tcof1* gene (Dixon et al., 2000). Both the HFM and TCS mutants exhibit asymmetric craniofacial defects, supporting a genetic origin for clinical craniofacial asymmetries. Unfortunately, few additional mutants with LR asymmetric craniofacial defects have been identified to date (Cousley et al., 2002). Characterization of a craniofacial asymmetry mutant (*ace/fgf8*) in the developmentally tractable zebrafish model system will facilitate the continuing effort to elucidate the developmental origins of clinical and naturally occurring facial asymmetries.

Evolutionary implications of craniodental laterality

Evidence of craniodental handedness also comes from nature, where a multitude of vertebrate taxa have elaborated asymmetries along the left–right (LR) axis in the head. For example, several species of African fruit bat exhibit asymmetric dental and craniofacial patterns (Juste and Ibanez, 1993; Juste et al., 2001). Narwhals display perhaps the most striking example of dental asymmetry with the left incisor growing up to 10 feet in males (Walker et al., 1968). Odontocete whales exhibit pronounced skull asymmetries associated with echolocation (Ness, 1967), and several owl taxa have independently evolved asymmetries in the size, shape and positioning of the external ear, which is thought to facilitate vertical location of sound/prey (Norberg, 1977). Flatfish display dramatic morphological and functional asymmetries, which are modifications for specialized prey-capture behaviors (Gibb, 1996). Finally, a clade of cichlid fishes from Lake Tanganyika has evolved craniodental asymmetries to more effectively strip scales from the left or right flank of prey species (Liem and Stewart, 1976). Strikingly, the frequency of left- or right-handed scale eaters within a population fluctuates over time, offering a consummate example of frequency-dependent natural selection (Hori, 1993).

In most cases, the adaptive advantage conferred by accentuating LR asymmetries is clear (e.g., handedness in scale eating cichlids). In other instances, the fixation of morphological asymmetry is presumably non-adaptive and likely the result of neutral processes such as genetic drift (e.g., dental asymmetry in fruit bats). In either situation, evolution has unmasked latent asymmetry in the developmental program. Our analysis of *fgf8* mutants has likewise revealed a fundamental asymmetry in zebrafish craniofacial development. It is possible that latent craniofacial asymmetry is a feature shared by all vertebrates. In the majority of taxa, it is masked by the wt function of craniofacial genes such as *fgf8*, whereas in more derived groups including flatfish and narwhals, craniofacial asymmetries are naturally expressed. Understanding how the LR axis is

determined and maintained during craniofacial development will facilitate an understanding of how natural selection has exploited positional identity along this axis.

Conclusions

Lateralization of the vertebrate body plan is both evolutionarily conserved and developmentally rigid. Conspicuous LR asymmetries are evident in a variety of tissues (brain, heart, lungs and gut). Moreover, a multitude of clinical disorders reveal underlying LR positional identity in superficially paired organs (e.g., hemifacial microsomia, hemihypertrophy) (Levin, 2005). These observations suggest a fundamental handedness to most, if not all structures, and raise the question of how many pathways are needed to specify (or modify) the LR axis during vertebrate development. That is to say, do unique molecular signaling pathways exist for each tissue type, or can all aspects of vertebrate laterality be traced to a single developmental origin (e.g., KV specification and morphogenesis)? Zebrafish LR asymmetry mutants offer a promising molecular foothold into elucidation of the molecular mechanisms directing vertebrate laterality.

Acknowledgments

We wish to thank members of the Yelick laboratory and Dr. Michael Levin for thoughtful comments on earlier versions of the manuscript, and Loic Fabricant and Seija Cope for expert zebrafish husbandry. This work was supported by NIDCR Grants DE12024 and DE12076 awarded to PCY. RCA is supported by a NIH T32 Postdoctoral Training Grant (T32 DE08327) awarded to The Forsyth Institute.

References

- Akimenko, M.A., Ekker, M., Wegner, J., Lin, W., Westerfield, M., 1994. Combinatorial expression of three zebrafish genes related to distal-less: part of a homeobox gene code for the head. *J. Neurosci.* 14, 3475–3486.
- Albertson, R.C., Yelick, P.C., 2004. Morphogenesis of the jaw: development beyond the embryo. In: Detrich, H.W., Zon, L., Westerfield, M. (Eds.), *The Zebrafish: Cellular and Developmental Biology, Methods in Cell Biology*, vol. 76. Elsevier, San Diego, CA, pp. 437–454.
- Amack, J.D., Yost, H.J., 2004. The T box transcription factor *no tail* in ciliated cells controls zebrafish left–right asymmetry. *Curr. Biol.* 14, 685–690.
- Bisazza, A., de Santi, A., 2003. Lateralization of aggression in fish. *Behav. Brain Res.* 141, 131–136.
- Bisgrove, B.W., Essner, J.J., Yost, H.J., 2000. Multiple pathways in the midline regulate concordant brain, heart and gut left–right asymmetry. *Development* 127, 3567–3579.
- Boettger, T., Wittler, L., Kessel, M., 1999. FGF8 functions in the specification of the right body side of the chick. *Curr. Biol.* 9, 277–280.
- Brueckner, M., 2001. Cilia propel the embryo in the right direction. *Am. J. Med. Genet.* 101, 339–344.
- Cassidy, K.M., Harris, E.F., Tolley, E.A., Keim, R.G., 1998. Genetic influence on dental arch form in orthodontic patients. *Angle Orthod.* 68, 445–454.
- Chen, J.N., Fishman, M.C., 1996. Zebrafish tinman homolog demarcates the heart field and initiates myocardial differentiation. *Development* 122, 3809–3816.
- Chen, J.N., van Eeden, F.J.M., Warren, K.S., Chin, A., Nüsslein-Volhard, C., Haffter, P., Fishman, M.C., 1997. Left–right pattern of cardiac BMP4 may drive asymmetry of the heart in zebrafish. *Development* 124, 4373–4382.
- Cooper, M.S., D’Amico, L.A., 1996. A cluster of non-involuting endocytic cells at the margin of the zebrafish blastoderm marks the site of embryonic shield formation. *Dev. Biol.* 180, 184–198.
- Corp, N., Byrne, R.W., 2004. Sex difference in chimpanzee handedness. *Am. J. Phys. Anthropol.* 123, 62–68.
- Cousley, R., Naora, H., Yokoyama, M., Kimura, M., Otani, H., 2002. Validity of the Hfm transgenic mouse as a model for hemifacial microsomia. *Cleft Palate–Craniofac. J.* 39, 81–92.
- Creuzet, S., Schule, B., Couly, G., Le Douarin, N.M., 2004. Reciprocal relationships between Fgf8 and neural crest cells in facial and forebrain development. *Proc. Natl. Acad. Sci. U. S. A.* 101, 4843–4847.
- Crump, J.G., Maves, L., Lawson, N.D., Weinstein, B.M., Kimmel, C.B., 2004. An essential role for Fgf8 in endoderm pouch formation influences later craniofacial skeletal patterning. *Development* 131, 5703–5716.
- Dixon, J., Brakebusch, C., Fassler, R., Dixon, M.J., 2000. Increased levels of apoptosis in the pre-fusion neural folds underlie the craniofacial disorder. Treacher Collins syndrome. *Hum. Mol. Genet.* 9, 1473–1480.
- Draper, B.W., Morcos, P.A., Kimmel, C.B., 2001. Inhibition of zebrafish *fgf8* pre-mRNA splicing with morpholino oligos: a quantifiable method for gene knockdown. *Genesis* 30, 154–156.
- Draper, B.W., Stock, D.W., Kimmel, C.B., 2003. Zebrafish *fgf24* functions with *fgf8* to promote posterior mesodermal development. *Development* 130, 4639–4654.
- Essner, J.J., Branford, W.W., Zhang, J., Yost, H.J., 2000. Mesoderm and left–right brain, heart and gut development are differentially regulated by *pitx2* isoforms. *Development* 127, 1081–1093.
- Essner, J.J., Vogan, K.J., Wagner, M.K., Tabin, C.J., Yost, H.J., Brueckner, M., 2002. Conserved function for embryonic nodal cilia. *Nature* 418, 37–38.
- Essner, J.J., Amack, J.D., Nyholm, M.K., Harris, E.B., Yost, H.J., 2005. Kupffer’s vesicle is a ciliated organ of asymmetry in the zebrafish embryo that initiates left–right development of the brain, heart and gut. *Development* 132, 1247–1260.
- Fischer, A., Viebahn, C., Blum, M., 2002. FGF8 acts as a right determinant during establishment of the left–right axis in the rabbit. *Curr. Biol.* 12, 1807–1816.
- Galaburda, A.M., LeMay, M., Kemper, T.L., Geschwind, N., 1978. Right–left asymmetries in the brain. *Science* 199, 852–856.
- Gibb, A.C., 1996. The kinematics of prey capture in *Xystreureys liolepis*: do all flatfish feed asymmetrically? *J. Exp. Biol.* 199, 2269–2833.
- Ghirlanda, S., Vallortigara, G., 2004. The evolution of brain lateralization: a game—Theoretical analysis of population structure. *Proc. R. Soc. Lond., B Biol. Sci.* 271, 853–857.
- Hall, B.K. (Ed.), 1999. *The Neural Crest in Development and Evolution*. Springer-Verlag, New York.
- Halpern, M.E., Liang, J.O., Gamse, J.T., 2003. Leaning to the left: laterality in the zebrafish forebrain. *Trends Neurosci.* 26, 308–313.
- Hamada, H., Meno, C., Watanabe, D., Saijoh, Y., 2002. Establishment of vertebrate left–right asymmetry. *Nat. Rev., Genet.* 3, 103–113.
- Hashimoto, H., Rebagliati, M., Ahmad, N., Muraoka, O., Kurokawa, T., Hibi, M., Suzuki, T., 2004. The Cerberus/Dan-family protein Charon is a negative regulator of Nodal signaling during left–right patterning in zebrafish. *Development* 131, 1741–1753.
- Hori, M., 1993. Frequency-dependent natural selection in the handedness of scale-eating cichlid fish. *Science* 260, 216–219.

- Jackman, W.R., Draper, B.W., Stock, D.W., 2004. Fgf signaling is required for zebrafish tooth development. *Dev. Biol.* 274, 139–157.
- Juste, J., Ibanez, C., 1993. An asymmetric dental formula in a mammal, the Sao Tome Island fruit bat *Myonycteris brachycephala* (Mammalia: Megachiroptera). *Can. J. Zool.* 71, 221–224.
- Juste, J., López-Gonzalez, C., Strauss, R.E., 2001. Analysis of asymmetries in the African fruit bats *Eidolon helvum* and *Rousettus aegyptiacus* (Mammalia: Megachiroptera) from the islands of the Gulf of Guinea: I. Variance and size components of bilateral variation. *J. Evol. Biol.* 14, 663–671.
- Kennedy, D.N., O'Craven, K.M., Ticho, B.S., Goldstein, A.M., Makris, N., Henson, J.W., 1999. Structural and functional brain asymmetries in human situs inversus totalis. *Neurology* 53, 1260–1265.
- Kimmel, C.B., Ballard, W.W., Kimmel, S.R., Ullmann, B., Schilling, T.F., 1995. Stages of embryonic development of the zebrafish. *Dev. Dyn.* 203, 253–310.
- Lazenby, R., 2002. Skeletal biology, functional asymmetry and the origins of “Handedness”. *J. Theor. Biol.* 218, 129–138.
- Leamy, L.J., Pomp, D., Eisen, E.J., Cheverud, J.M., 2000. Quantitative trait loci for directional but not fluctuating asymmetry of mandible characters in mice. *Genet. Res.* 76, 27–40.
- Levin, M., 1999. Twinning and embryonic left–right asymmetry. *Laterality* 4, 197–208.
- Levin, M., 2005. Left-right asymmetry in embryonic development: a comprehensive review. *Mech. Dev.* 122, 3–25.
- Levin, M., Mercola, M., 1998. Gap junctions are involved in the early generation of left–right asymmetry. *Dev. Biol.* 203, 90–105.
- Levin, M., Mercola, M., 1999. Gap junction-mediated transfer of left–right patterning signals in the early chick blastoderm is upstream of Shh asymmetry in the node. *Development* 126, 4703–4714.
- Liang, J.O., Etheridge, A., Hantsoo, L., Rubinstein, A.L., Nowak, S.J., Izpisúa Belmonte, J.C., Halpern, M.E., 2000. Asymmetric Nodal signaling in the zebrafish diencephalon positions the pineal organ. *Development* 127 (23), 5101–5112.
- Liem, K.F., Stewart, D.J., 1976. Evolution of the scale-eating cichlid fishes of Lake Tanganyika: a generic revision with a description of a new species. *Bull. Mus. Comp. Zool.* 147, 319–350.
- Lister, J.A., Robertson, C.P., Lepage, T., Johnson, S.L., Raible, D.W., 1999. *nacre* encodes a zebrafish microphthalmia-related protein that regulates neural-crest-derived pigment cell fate. *Development* 126, 3757–3767.
- Long, S., Ahmad, N., Rebagliati, M., 2003. The zebrafish nodal-related gene *southpaw* is required for visceral and diencephalic left–right asymmetry. *Development* 130, 2303–2316.
- Mercola, M., Levin, M., 2001. Left–right asymmetry determination in vertebrates. *Annu. Rev. Cell. Dev. Biol.* 17, 779–805.
- Meyers, E.N., Martin, G.R., 1999. Differences in left–right axis pathways in mouse and chick: functions of FGF8 and SHH. *Science* 285, 403–406.
- Naora, H., Kimura, M., Otani, H., Yokoyama, M., Koizumi, T., Katsuki, M., Tanaka, O., 1994. Transgenic mouse model of hemifacial microsomia: cloning and characterization of insertional mutation region on chromosome 10. *Genomics* 23, 515–519.
- Ness, A.R., 1967. A measure of asymmetry of the skulls of odontocete whales. *J. Zool. Lond.* 153, 209–221.
- Nonaka, S., Shiratori, H., Saijoh, Y., Hamada, H., 2002. Determination of left–right patterning of the mouse embryo by artificial nodal flow. *Nature* 418, 96–99.
- Norberg, R.A., 1977. Occurrence and independent evolution of bilateral asymmetry in owls and implications on owl taxonomy. *Philos. Trans. R. Soc. London, B* 280, 375–408.
- Piotrowski, T., Nusslein-Volhard, C., 2000. The endoderm plays an important role in patterning the segmented pharyngeal region in zebrafish (*Danio rerio*). *Dev. Biol.* 225, 339–356.
- Pothoff, T., 1984. Clearing and staining techniques. In: Moser, H.G., Richards, W.J., Cohen, D.M., Fahay, M.P., Kendall, A.W., Richardson, S.L. (Eds.), *Ontogeny and Systematics of Fishes*. American Society of Ichthyologists and Herpetologists, Lawrence, KS, pp. 35–37.
- Reifers, F., Bohlh, H., Walsh, E.C., Crossley, P.H., Stainier, D.Y., Brand, M., 1998. *Fgf8* is mutated in zebrafish *acerebellar* (*ace*) mutants and is required for maintenance of midbrain–hindbrain boundary development and somitogenesis. *Development* 125, 2381–2395.
- Reifers, F., Walsh, E.C., Léger, S., Stainier, D.Y.R., Brand, M., 2000. Induction and differentiation of the zebrafish heart requires fibroblast growth factor 8 (*fgf8/acerebellar*). *Development* 127, 225–235.
- Sagerstrom, C.G., Grimbalt, Y., Sive, H., 1996. Anteroposterior patterning in the zebrafish, *Danio rerio*: an explant assay reveals inductive and suppressive cell interactions. *Development* 122, 1873–1883.
- Schulte-Merker, S., van Eeden, F.J.M., Halpern, M.E., Kimmel, C.B., Nusslein-Volhard, C., 1994. *No tail* (*ntl*) is the zebrafish homologue of the mouse *T* (*Brachyury*) gene. *Development* 120, 1009–1015.
- Thesleff, I., Vaahtokari, A., Partanen, A.M., 1995. Regulation of organogenesis. Common molecular mechanisms regulating the development of teeth and other organs. *Int. J. Dev. Biol.* 39, 35–50.
- Thisse, C., Thisse, B., Schilling, T.F., Postlethwait, J.H., 1993. Structure of the zebrafish *snail1* gene and its expression in wild-type, *spadetail* and *no tail* mutant embryos. *Development* 119, 1203–1215.
- Thisse, B., Pflumio, S., Fürthauer, M., Loppin, B., Heyer, V., Degraeve, A., Woehl, R., Lux, A., Steffan, T., Charbonnier, X.Q., Thisse, C., 2001. Expression of the zebrafish genome during embryogenesis (NIH R01 RR15402). ZFIN Direct Data Submission.
- Tiner, B.D., Quaroni, A.L., 1996. Facial asymmetries in hemifacial microsomia, Goldenhar syndrome, and Treacher Collins syndrome. *Atlas Oral Maxillofac. Surg. Clin. N. Am.* 4, 37–52.
- Walker, E.P., Warnick, F., Hamlet, S.E., Lange, K.I., Davis, M.A., Uible, H.E., Wright, P.F. (Eds.), 1968. *Mammals of the World*, 2nd ed. The Johns Hopkins Press, Baltimore.
- Walshe, J., Mason, I., 2003. *Fgf* signaling is required for formation of cartilage in the head. *Dev. Biol.* 264, 522–536.
- Westerfield, M. (Ed.), 1995. *The Zebrafish Book. A Guide for the Laboratory Use of Zebrafish (Danio rerio)*, 3rd ed. Univ. of Oregon Press, Eugene.
- Zhu, L., Marvin, M.J., Gardiner, A., Lassar, A.B., Mercola, M., Stern, C.D., Levin, M., 1999. Cerberus regulates left–right asymmetry of the embryonic head and heart. *Curr. Biol.* 9, 931–938.